Preparation and Optoelectronic Properties of a Novel Poly(*N*-vinylcarbazole) with Covalently Bonded Titanium Dioxide

Yangang Han, Gang Wu, Hongzheng Chen, Mang Wang

Department of Polymer Science and Engineering, State Key Laboratory of Silicon Materials, Key Laboratory of Macromolecule Synthesis and Functionalization (Ministry of Education), Zhejiang University, Hangzhou 310027, People's Republic of China

Received 13 August 2007; accepted 21 January 2008
DOI 10.1002/app.28110
Published online 10 April 2008 in Wiley InterScience (www.interscience.wiley.com).

ABSTRACT: A functional organic–inorganic composite containing carbazole moieties (electron donors) and TiO_2 (electron acceptors) in different molar ratios, TiO_2-modified poly(*N*-vinylcarbazole) (PVK–TiO_2), was synthesized through a nucleophilic reaction. The molecular and electronic structure of the PVK–TiO_2 composite was characterized with Fourier transform infrared, ultraviolet–visible absorption, cyclic voltammetry, and so forth. The highest occupied molecular orbital and lowest unoccupied molecular orbital energy levels of the PVK–TiO_2 composite were higher than those of pristine poly(*N*-vinylcarbazole). The PVK–TiO_2 composite exhibited an enhanced glass-transition temperature and improved thermal stability. The photoinduced charge transfer observed in photofluorescence and photoconductivity measurements makes applications in the field of photodetectors possible. The PVK–TiO_2 composite containing carbazole moieties and TiO_2 in a molar ratio of about 58 : 1 was found to have the best photosensitivity. © 2008 Wiley Periodicals, Inc. J Appl Polym Sci 109: 882–888, 2008

Key words: charge transfer; composites; fluorescence; functionalization of polymers

INTRODUCTION

Because of the advantages implied for polymer-based electronics, including low-cost fabrication in large areas, high mechanical flexibility, and the versatility of the chemical structure, conjugated polymers have been investigated for many years as photoactive components in solar cells,[1–4] photodetectors,[5] light-emitting diodes,[6–8] and memory devices.[9,10] Since the discovery of the photoconduction of poly(*N*-vinylcarbazole) (PVK) in 1957, PVK has become one of the best photoconductive polymers for electronic and optical applications because of its effective hole-transport ability[11] and relatively high glass-transition temperature (T_g).[12] Like most photoconductive polymers, electron transport in PVK is nearly completely retarded because of effective trapping by oxygen and oxidative impurities.[13]

To date, the exploitation of PVK as an active material component has occurred mainly with doped PVK or PVK blends.[14–16] Meanwhile, work on the chemical modification of PVK has been done in recent years. Wang et al.[17] functionalized PVK with single-walled carbon nanotubes. PVK with covalently bonded fullerene was synthesized by Ling et al.[8]

Semiconductor nanoparticles, which exhibit properties different from those of bulk materials, are attractive materials that hold considerable potential for numerous applications in the fields of electronics and photonics. TiO_2 on the nanometer scale has been widely studied as a semiconductor substrate for dye-sensitized solar cells.[18–21] Efficient interface charge separation/transfer can be expected from advantages such as the large surface area to volume ratio, the low potential of the conduction band edge, and the high state density of the conduction band.[22]

The design and synthesis of a processable polymer that can provide the required electronics properties within a single macromolecule and yet still possesses good chemical, mechanical, and morphological characteristics are desired for optoelectronic devices. Our functionalization method of PVK reported in this article is based on the nucleophilic reaction of

Correspondence to: H. Z. Chen (hzchen@zju.edu.cn) or M. Wang (mwang@zju.edu.cn)

Contract grant sponsor: National Natural Science Foundation of China; contract grant numbers: 50433020, 50503021, 50773067 and 50520150165.

Contract grant sponsor: Changjiang Scholar and Innovation Team (Ministry of Education of China); contract grant number: IRT0651.

Contract grant sponsor: Fund for the Major State Basic Research Development Program; contract grant number: 2007CB613400.

polymeric carbanions, which are generated by α-position proton abstraction with sodium hydride.[23] TiO_2 nanoparticles are amphoteric in nature, and the charge can be controlled by the adjustment of the pH of the colloidal suspension below or above the isoelectric point (I_p) of TiO_2.[24] In principle, I_p of an aqueous colloidal TiO_2 dispersion varies from 4.5 to 6.8.[25] If the pH of the medium is higher than I_p of TiO_2, the surface charge of TiO_2 particles is negative. If the medium pH is lower than I_p of TiO_2, the particles are positively charged. Therefore, by the simple adjustment of the medium pH, the TiO_2 nanoparticles can be specifically charged to positive. In this work, PVK with different contents of covalently bonded TiO_2 has been synthesized and characterized. In this modified polymer, the carbazole moieties serve as the electron donor and hole-transporting moiety,[8] and TiO_2 plays a dual role as both an electron acceptor and an electron conductor.[26]

EXPERIMENTAL

PVK (weight-average molecular weight = 90,000), purchased from Acros (Geel, Belgium), was used as received. Sodium hydride was purchased from Fluka (Buchs, Switzerland). Tetrabutylammonium perchlorate (TBAP) was obtained from Acros and baked *in vacuo* at 120°C for 4 h before use. Acetonitrile was refluxed over CaH_2 for 2 h and distilled under reduced pressure. Toluene and tetrahydrofuran (THF) were refluxed over sodium in the presence of benzophenone until a persistent blue color appeared and were then distilled before use. All of the glassware was prebaked at 120°C, cooled *in vacuo*, and purged with pure N_2 (99.99%).

The synthetic route of TiO_2-functionalized PVK is shown in Scheme 1 and is based on a similar method in the literature.[23] A mixture of PVK (1.0 g) and sodium hydride (0.2 g) was dissolved in 30 mL of dry THF and stirred at room temperature for 24 h in a glovebox filled with pure N_2. Different amounts of tetrabutyltitanate (TBT), that is, 0.24, 0.49, and 1.20 g, were added to 60 mL of dry toluene and stirred for 1.5 h. An appropriate amount of acetic acid was added to the solution to give a molar ratio of CH_3COOH/Ti = 1.2 for all samples. Acetic acid was a catalyst for the hydrolysis and condensation of the TiO_2 precursor. Also, it was used to adjust the pH value of the reaction medium. Under acidic conditions, TiO_2 was charged positively and could be bonded to the negatively charged PVK. Then, the solution was placed in an oven saturated with water vapor for a hydrolysis reaction for 1.5 h at 40°C. Because the pH of our sol system was much lower than I_p of TiO_2, the nanoparticles were charged positively. The TiO_2 sol (45 mL) was dropwise added to the polymer solution over a period of 1.5 h, and this

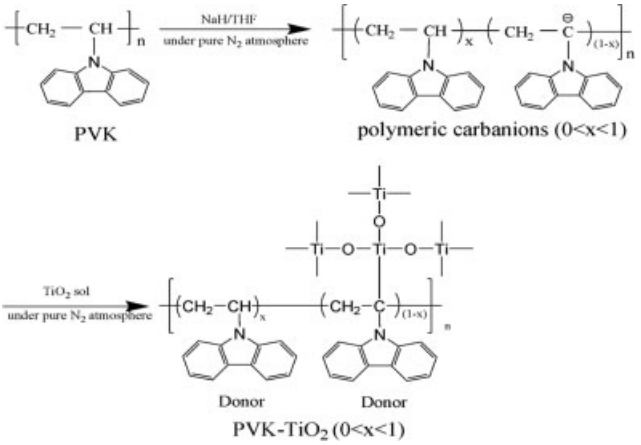

Scheme 1 Synthetic route and molecular structure of PVK–TiO_2 composites.

was followed by vigorous stirring at room temperature for 72 h; it then settled for 12 h. The resulting solution was precipitated into an excess amount of methanol in which TiO_2 could dissolve under vigorous stirring. The precipitate was collected by filtration through the polytetrafluoroethylene membrane and washed with a mixed solvent of methanol and benzene (100 : 1 v/v) three times. The polymer was redissolved in *o*-dichlorobenzene and filtered to remove the unreacted TiO_2 because the solubility of TiO_2 in *o*-dichlorobenzene could be neglected. TiO_2-modified poly(*N*-vinylcarbazole) (PVK–TiO_2) was reprecipitated from methanol and dried at 60°C *in vacuo* overnight.

Fourier transform infrared (FTIR) spectra were measured on a Bruker Vector 22 (Ettlingen, Germany) spectrometer with KBr pressed discs. Ultraviolet–visible (UV–vis) spectra were recorded on a Varian Cary 100 biospectrometer (Palo Alto, CA). Cyclic voltammetry (CV) measurements were performed on a CHI600A electrochemical workstation (Shanghai Chenhua Instrument Company, Shanghai, China) with a three-electrode cell under an N_2 atmosphere. The polymer film on a Pt disk electrode (working electrode) was scanned anodically in a solution of TBAP in acetonitrile (0.1*M*) with a saturated calomel electrode and a platinum wire as the reference and counter electrodes, respectively. Thermogravimetric analysis (TGA) was conducted on a TA Instruments (New Castle, DE) SDT Q600 thermogravimetric analyzer under air at a heating rate of 20°C/min. Differential scanning calorimetry (DSC) was measured on a TA Instruments DSC Q100 system under N_2 and at a heating rate of 10°C/min. Elemental analysis was carried out on a ThermoFinnigan Flash EA1112 elemental analyzer (Silicon Valley, CA). Room-temperature fluorescence spectra were recorded on a PerkinElmer (Waltham, MA) LS55 luminescence spectrometer. Photoconductivity was measured with the standard photoinduced

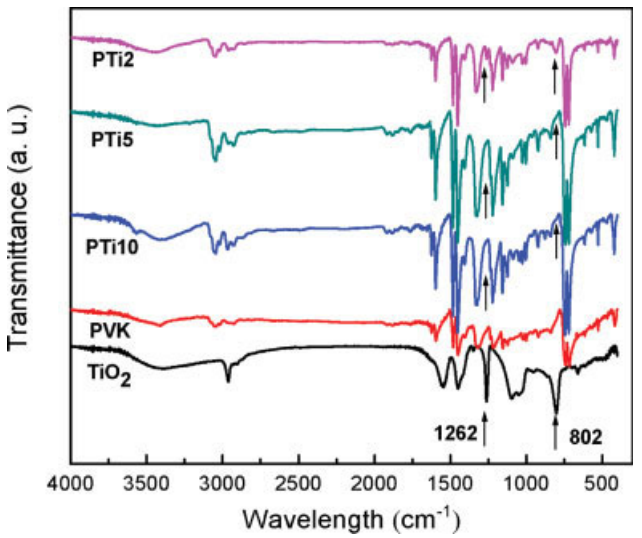

Figure 1 FTIR spectra of as-prepared TiO_2, pristine PVK, and PVK–TiO_2 composites with different TiO_2 concentrations. [Color figure can be viewed in the online issue, which is available at www.interscience.wiley.com.]

discharge method on the GDT-II model photoconductivity measuring device with a 500-W Xe lamp with a filter as a UV light source. The electrode substrate, an aluminum plate, was coated with a poly (methyl methacrylate) charge blocking layer. The pristine PVK and functionalized PVK served as the charge generation layer, onto which a charge transportation layer of a polycarbonate matrix containing 10 wt % *N*,*N*′-diethyl-4-aminobenzaldehyde-1,1′-diphenylhydrozone was coated; this gave a double-layered photoreceptor.

RESULTS AND DISCUSSION

Synthesis and chemical characterization

Figure 1 presents the FTIR spectra of PVK, TiO_2, and PVK–TiO_2, and the characteristic absorption bands at 751 and 725 cm^{-1} (doublet) for the carbazole group can be found. As indicated in Table I, PTi10, PTi5, and PTi2 were used to label the samples with different amounts of added TBT. In addition to the vibration absorption of alkyl and aryl groups in PVK, in the plot of PTi2, the peaks at 1262 and 802 cm^{-1}, associated with TiO_2, are also discernible with the increased concentration of TiO_2, and this is an indication of the successful modification of PVK.[27] However, these two peaks are too weak to be observed in plots of PTi5 and PTi10 because of the low loadings of TiO_2 in the composites.

As shown in Table I, the components of the composition were verified by elemental analysis. The content of carbazole moieties can be calculated from the N element, and that of TiO_2 can be calculated from the other elements, except for the systematic error. The value of 0.57 was the systematic error in measuring the elemental components of pristine PVK. Here, as a convenience, it is assumed that the systematic error is constant in the elemental analysis. Although it is not an exactly quantitative method, it indicates the changes in the components of the composites. Thus, the ratios of the number of carbazole moieties to the number of TiO_2 [n(carbazole)/n(TiO_2)] could be obtained, and they are listed in Table I.

Thermal properties of the PVK–TiO_2 composites

Figure 2 presents the thermal stability of PVK and PVK–TiO_2 composites with different concentrations of TiO_2. In comparison with their homopolymer counterpart, all the PVK–TiO_2 composites started to degrade at a higher temperature (Table II), and this indicated that the thermal stability of PVK was enhanced by the covalent bonding of TiO_2 onto the polymer chain.

As shown in Figure 3, T_g of pristine PVK is about 190°C. After the covalent bonding of TiO_2, because the mobility of the polymer chain is restricted by steric hindrance caused by TiO_2, T_g of the composites increases to about 230°C. However, some of the small TiO_2 particles can function as plasticizers, so T_g does not increase along with the increase in the TiO_2 concentration. The relatively high T_g of this polymer–TiO_2 hybrid will be advantageous to its application as an active material in an electronic device.

To distinguish physical blending and chemical modification, we also prepared blends of PVK and as-prepared TiO_2. It can be observed in Figure 3 that the DSC curve of the blends is similar to that of pure PVK and different from that of PVK–TiO_2 composites. It can be concluded that chemical modification of PVK has been achieved successfully.

TABLE I
Elemental Analysis of Pristine PVK and PVK–TiO_2 Composites with Different TiO_2 Concentrations

Sample	TBT (g)	C (%)	H (%)	N (%)	Others (%)		n(carbazole)/n (TiO_2)
					Systematic error	Ti and O	
PVK	0	86.37	5.75	7.31	0.57	0	—
PTi10	0.24	86.27	5.77	7.24	0.57	0.15	276
PTi5	0.49	85.74	5.78	7.20	0.57	0.71	58
PTi2	1.20	83.24	5.86	6.94	0.57	2.89	14

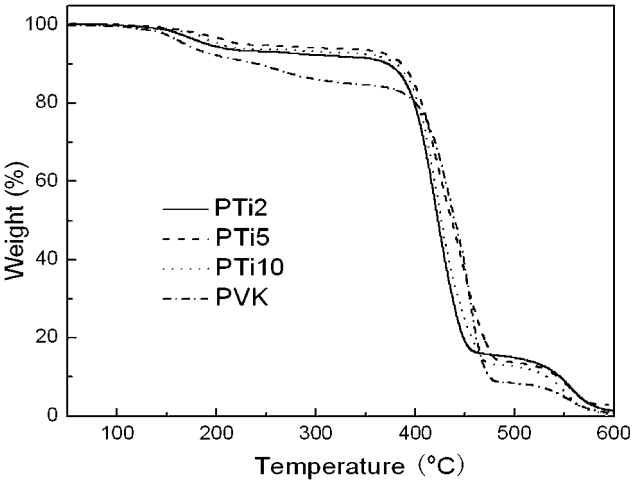

Figure 2 TGA curves of pristine PVK and PVK–TiO_2 composites with different TiO_2 concentrations.

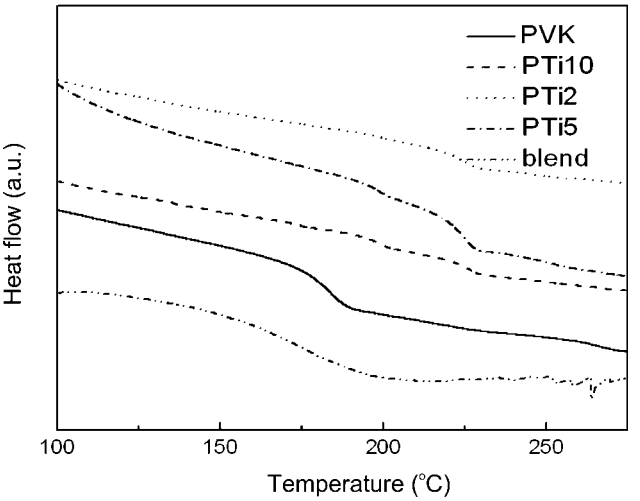

Figure 3 DSC curves of pristine PVK, a PVK/TiO_2 blend, and PVK–TiO_2 composites with different TiO_2 concentrations.

Absorption properties and photoluminescence (PL) characteristics

The UV–vis spectra of PVK–TiO_2 composites in THF solutions are shown in Figure 4 together with those of pristine PVK and as-prepared TiO_2. Besides three absorption peaks at 294, 330, and 343 nm for the pristine PVK, TiO_2 is responsible for the absorption band around 288 nm in the PVK–TiO_2 system. The weakness and broadness of the peak may be due to a relatively low concentration of TiO_2 along with the strong absorption of PVK in the UV region.

CV is an effective method for exploring the relative ionization and reduction potential (P_{ir}). The highest occupied molecular orbital energy level (E_{HOMO}) was calculated with the following equation:

$$E_{HOMO} = -|P_{ir}| = -|eE_{1/2} + 4.5\,eV + E_{sce}|$$
$$= -|eE_{1/2} + 4.741\,eV|$$

where E_{sce} is the energy level of the standard calomel electrode.

Combined with the band gap (E_g) obtained from UV–vis results, the lowest unoccupied molecular orbital energy level (E_{LUMO}) was also calculated as follows:

$$E_{LUMO} = E_g + E_{HOMO}$$

The results are listed in Table III.

When PVK was covalently modified with TiO_2, because a p–n heterojunction formed and band bending occurred in the interface,[28] the highest occupied molecular orbital (HOMO) and lowest unoccupied molecular orbital (LUMO) levels for PVK–TiO_2 composites were enhanced in comparison with those of pristine PVK. In an n-type material, the Fermi level is closer to the bottom of the conduction band, whereas in a p-type material, it is closer to the top of the valence band. If these n-type and p-type semi-

TABLE II
Thermal Stability of Pristine PVK and PVK–TiO_2 Composites

Sample	T_d (°C)[a]
PVK	169
PTi10	205
PTi5	205
PTi2	202

[a] Temperature of 5% weight loss.

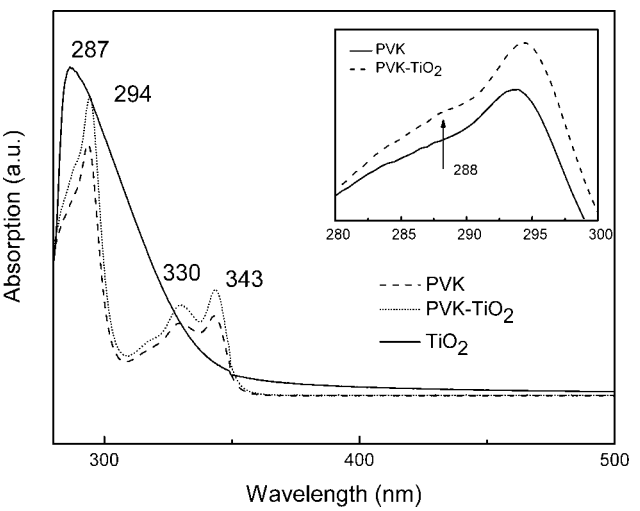

Figure 4 UV–vis absorption spectra of as-prepared TiO_2, pristine PVK, and PVK–TiO_2 composites.

TABLE III
HOMO Energy Levels, LUMO Energy Levels (vs the Vacuum Level), and E_g Values of Pristine PVK and PVK–TiO_2 Composites

Sample	HOMO (eV)	LUMO (eV)	E_g (eV)
PVK	−6.03	−2.50	3.53
PTi10	−5.82	−2.28	3.54
PTi5	−5.80	−2.27	3.53
PTi2	−5.79	−2.25	3.54

conductors are brought into contact, according to the following equation, electric current will flow if the Fermi level is not constant through the whole system:

$$j = \mu_n n \frac{dE_{Fn}}{dx} + \mu_p p \frac{dE_{Fp}}{dx}$$

where j is the current density, μ_n is the electron mobility, μ_p is the hole mobility, n is the electron concentration, p is the hole concentration, E_{Fn} is the Fermi level of an n-type material, E_{Fp} is the Fermi level of a p-type material, and x is the space coordinate.

Hence, under equilibrium conditions, the Fermi level must be constant throughout the whole sample, and this means that E_{Fn} and E_{Fp} are equal to each other. For $E_{Fn} \neq E_{Fp}$ before equilibrium, the requirement of the constancy of the Fermi level leads to the status presented by the energy band diagram shown in Figure 5. It will be recalled that a p-type semiconductor causes the band energy levels to move up with respect to the Fermi level and that the presence of an n-type semiconductor causes the band energy levels to move down,[29] and this accounts for the enhancement of the HOMO and LUMO levels of PVK–TiO_2 composites.

The PL measurements given in Figure 6 indicate that the excitons in the polymer were visibly quenched with the increase in the TiO_2 concentration. Charge transfer led to quenching of PL because the photogenerated excitons were dissociated before luminescence could occur.[30] According to the integrated area beneath each curve,[31] the quenching efficiencies of PTi10, PTi5, and PTi2 were found to be 55.8, 57.8,and 48.9%, respectively. A low ratio of TiO_2 would result in an insufficient number of acceptors to hold the charges. However, the quenching efficiency dropped for PTi2 even though TiO_2 acted as an acceptor for the photoinduced electrons generated in the polymer phase, perhaps because the total surface area of TiO_2 fell as the oxide particles aggregated but less as the TiO_2 content increased; this reduced the area of the donor/acceptor interface and the efficiency of the photoinduced transfer of electrons.[32] Besides, the broad peak around 420 nm agreed with the PL of TiO_2 nanoparticles,[33] which was also found in our as-prepared TiO_2 nanoparticles.

Photoconductivity properties

The photosensitivity is expressed as $(E_{1/2})^{-1}$:

$$E_{1/2} = I \times t_{1/2}$$

where $E_{1/2}$ is the energy needed when the potential reduces to the half under illumination, I is the light intensity and $t_{1/2}$ is the time from the initial potential to half the potential under illumination. Figure 7 presents the photosensitivity of photoreceptors constructed of PVK and functionalized PVK, respectively. The photoconductivity of the latter was higher than that of the former. That is, the addition

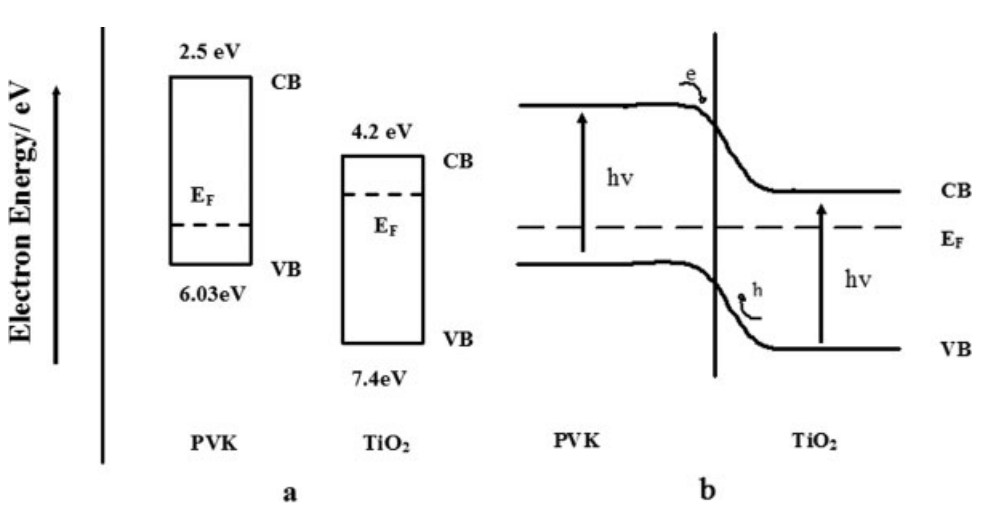

Figure 5 Energy band diagrams of (a) PVK and TiO_2 and (b) PVK–TiO_2 composites. CB, VB, and E_F denote the conduction band, valence band, and Fermi level, respectively.

of TiO_2 helped to improve the photosensitivity of the device. The dependence of the photosensitivity on the content of TiO_2 coincided well with the variation of the quenching efficiencies.

In general, the enhancement of illumination will increase the number of photogenerated excitons in materials. PVK is a p-type semiconductor with absorption in the UV region. A large interface area between PVK and TiO_2 could be achieved in functionalized PVK with covalently bonded TiO_2. When the photoreceptor was exposed to UV light ranging from 280 to 420 nm, PVK acted as a charge generation material, and the excitons generated in PVK moved to the large interface between TiO_2 and PVK for separation. The free electrons were injected into the conducting band of TiO_2 and diffused/drifted to the anode. The increased photosensitivity resulted from the efficient separation of excitons due to the large interface between PVK and TiO_2 as well as the convenient transport of free charges to the corresponding electrodes.

CONCLUSIONS

A series of PVKs with different concentrations of covalently bonded TiO_2 were synthesized by a nucleophilic reaction. The HOMO and LUMO energy levels of PVK–TiO_2 composites were higher than those of pristine PVK because of the band bending in the interface. Along with improved thermal stability, photoinduced charge transfer was deduced from photofluorescence and photoconductivity results, and this makes the composites promising candidates in the area of photodetectors. The best photosensitivity was found for the PVK–TiO_2 composite containing carbazole moieties and TiO_2 in a molar ratio of about 58 : 1. Further studies on the photoconductive properties of PVK–TiO_2 composites are currently underway.

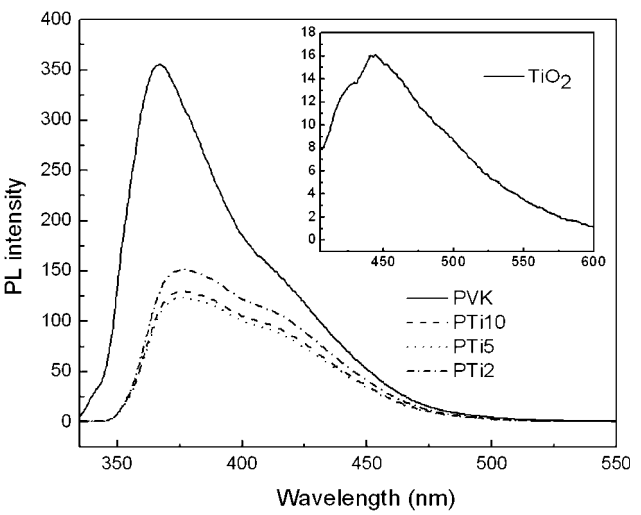

Figure 6 PL spectra of pristine PVK and PVK–TiO_2 composites with different TiO_2 concentrations (excited at 340 nm, 10^{-4} g/mL solution in THF). The inset shows the PL spectrum of as-prepared TiO_2.

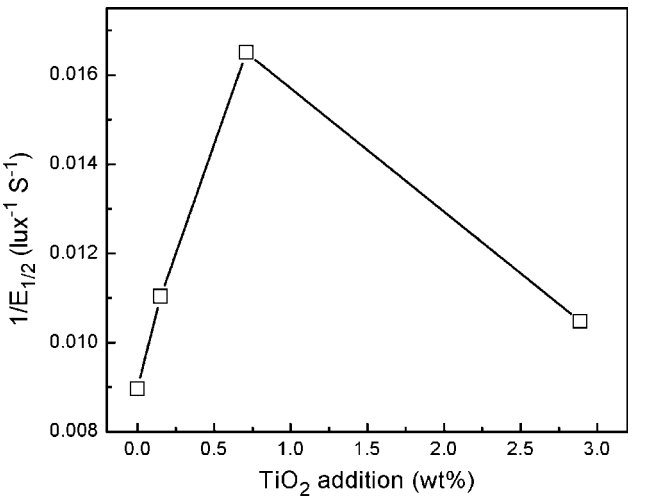

Figure 7 Photosensitivity of photoreceptors constructed of pristine PVK and PVK–TiO_2 composites with different TiO_2 concentrations (under an illumination of 3 mW/cm^2 UV light ranging from 280 to 420 nm).

References

1. Wang, Y. Nature 1992, 356, 585.
2. Yu, G.; Gao, J.; Hummelen, J. C.; Wudl, F.; Heeger, A. J. Science 1995, 270, 1789.
3. Shao, Y.; Bazan, G. C.; Heeger, A. J. Adv Mater 2007, 19, 365.
4. McDonald, S. A.; Cyr, P. W.; Levina, L.; Sargent, E. H. Appl Phys Lett 2004, 85, 2089.
5. Yang, X. N.; Loos, J. Macromolecules 2007, 40, 1353.
6. Gupta, D.; Kabra, D.; Kolishetti, N.; Ramakrishnan, S.; Narayan, K. S. Adv Funct Mater 2007, 17, 226.
7. Niu, Y. H.; Liu, M. S.; Ka, J. W.; Bardeker, J.; Zin, M. T.; Schofield, R.; Chi, Y.; Jen, A. K. Y. Adv Mater 2007, 19, 300.
8. Ling, Q. D.; Lim, S. L.; Song, Y.; Zhu, C. X.; Chan, N. S. H.; Kang, E. T.; Neoh, K. G. Langmuir 2007, 23, 312.
9. Yamaura, J.; Muraoka, Y.; Yamauchi, T.; Muramatsu, T.; Hiroi, Z. Appl Phys Lett 2003, 83, 2097.
10. Ouyang, J. Y.; Chu, C. W.; Scmanda, C. R.; Ma, L. P.; Yang, Y. Nat Mater 2004, 3, 918.
11. Wang, S. H.; Zeng, Z. H.; Yang, S. H.; Weng, L. T.; Wong, P. C. L.; Ho, K. C. Macromolecules 2000, 33, 3232.
12. Bergford, J. A.; Penwell, R. C.; Stolka, M. J Polym Sci Polym Phys Ed 1979, 17, 711.
13. Winiarz, J. G.; Zhang, L. M.; Lal, M.; Friend, C. S.; Prasad, P. N. Chem Phys 1999, 245, 417.
14. Xuan, Y.; Pan, D. C.; Zhao, N. N.; Ji, X. L.; Ma, D. G. Nanotechnology 2006, 17, 4966.
15. Wu, W.; Li, J. X.; Yang, L. M.; Guo, Z. X.; Dai, L. M.; Zhu, D. B. Chem Phys Lett 2002, 364, 196.
16. Jin, H.; Hou, Y. B.; Meng, X. G.; Teng, F. Chem Phys 2006, 330, 501.
17. Wang, W.; Lin, Y.; Sun, Y. P. Polymer 2005, 46, 8634.
18. O'Regan, B.; Gratzel, M. Nature 1991, 353, 737.
19. Liang, L. Y.; Dai, S. Y.; Hu, L. H.; Kong, F. T.; Xu, W. W.; Wang, K. J. J Phys Chem 2006, 110, 12404.
20. Beltran, E. L.; Prene, P.; Boscher, C.; Belleville, P.; Buvat, P.; Sanchez, C. Adv Mater 2006, 18, 2579.

21. O'Hayre, R.; Nanu, M.; Schoonman, J.; Goossens, A.; Wang, Q.; Gratzel, M. Adv Funct Mater 2006, 16, 1566.
22. Yang, J. H.; Warren, D. S.; Gordon, F. C.; McQuillan, A. J. J Appl Phys 2007, 101, 023714-1.
23. Chen, Y.; Chen, S. M.; Xiao, L. X.; Cai, R. F.; Huang, Z. E. J Mater Sci 1998, 33, 2061.
24. He, J. A.; Mosurkal, R.; Samuelson, L. A.; Li, L.; Kumar, J. Langmuir 2003, 19, 2169.
25. Liu, Y. J.; Wang, A. B.; Claus, R. J Phys Chem B 1997, 101, 1385.
26. Xie, Z. B.; Henry, B. M.; Kirov, K. R.; Barkhouse, D. A.; Burlakov, V. M.; Smith, H. E.; Grovenor, C. R.; Assender, H. E.; Briggs, G. A. D.; Kano, M.; Tsukahara, Y. Nanotechnology 2007, 18, 145708.
27. Connor, P. A.; Dobson, K. D.; McQuillan, A. J. Langmuir 1999, 15, 2402.
28. Mo, X.; Chen, H. Z.; Wang, Y.; Shi, M. M.; Wang, M. J Phys Chem B 2005, 109, 7659.
29. Burford, W. B.; Verner, H. G. Semiconductor Junctions and Devices; McGraw-Hill: New York, 1965; p 51.
30. Wang, P.; Abrusci, A.; Wong, H. M.; Svensson, M.; Anderson, M. R.; Greenham, N. C. Nano Lett 2006, 6, 1789.
31. Lin, Y. J.; Wang, L.; Chiu, W. Y. Thin Solid Films 2006, 511, 199.
32. Ji, J. S.; Lin, Y. J.; Lu, H. P.; Wang, L.; Rwei, S. P. Thin Solid Films 2006, 511, 182.
33. Abazovic, N. D.; Comor, M. I.; Dramicanin, M. D.; Jovanovic, D. J.; Ahrenkiel, S. P.; Nedeljkovic, J. M. J Phys Chem B 2006, 110, 25366.